

# Gene Correction of Integrin $\beta_4$ -dependent Pyloric Atresia-Junctional Epidermolysis Bullosa Keratinocytes Establishes a Role for $\beta_4$ Tyrosines 1422 and 1440 in Hemidesmosome Assembly\*

Received for publication, April 9, 2001, and in revised form, August 22, 2001  
Published, JBC Papers in Press, August 24, 2001, DOI 10.1074/jbc.M103139200

Elena Dellambra‡, Silvia Prislei‡, Anna Laura Salvati‡, Maria Luisa Madeddu‡, Osvando Golisano‡, Emanuela Siviero‡, Sergio Bondanza‡, Sandra Cicuzza§, Angela Orecchia§, Filippo G. Giancotti¶, Giovanna Zambruno§, and Michele De Luca‡||

From the ‡Laboratory of Tissue Engineering and §Laboratory of Molecular and Cellular Biology, Istituto Dermopatico dell'Immacolata, 00167 Rome, Italy and ¶Cellular Biochemistry and Biophysics Program, Memorial Sloan-Kettering Cancer Center, New York, New York

The cytoplasmic domain of  $\beta_4$  integrin contains two pairs of fibronectin-like repeats separated by a connecting segment. The connecting segment harbors a putative tyrosine activation motif in which tyrosines 1422 and 1440 are phosphorylated in response to  $\alpha_6\beta_4$  binding to laminin-5. Primary  $\beta_4$ -null keratinocytes, obtained from a newborn suffering from lethal junctional epidermolysis bullosa, were stably transduced with retroviruses carrying a full-length  $\beta_4$  cDNA or a  $\beta_4$  cDNA with phenylalanine substitutions at Tyr-1422 and Tyr-1440. Hemidesmosome assembly was evaluated on organotypic skin cultures.  $\beta_4$ -corrected keratinocytes were indistinguishable from normal cells in terms of  $\alpha_6\beta_4$  expression, the localization of hemidesmosome components, and hemidesmosome structure and density, suggesting full genetic and functional correction of  $\beta_4$ -null keratinocytes. In cultures generated from  $\beta_4^{Y1422F/Y1440F}$  keratinocytes,  $\beta_4$  mutants as well as  $\alpha_6$  integrin, HD1/plectin, and BP180 were not concentrated at the dermal-epidermal junction. Furthermore, the number of hemidesmosomes was strikingly reduced as compared with  $\beta_4$ -corrected keratinocytes. The rare hemidesmosomes detected in  $\beta_4^{Y1422F/Y1440F}$  cells were devoid of sub-basal dense plates and of inner cytoplasmic plaques with keratin filament insertion. Collectively, our data demonstrate that the  $\beta_4$  tyrosine activation motif is not required for the localization of  $\alpha_6\beta_4$  at the keratinocyte plasma membrane but is essential for optimal assembly of *bona fide* hemidesmosomes.

Human epidermis consists of a stratified squamous epithelium composed of keratinocytes organized in distinct cellular layers. Keratinocytes forming the basal layer firmly adhere to the basement membrane by means of hemidesmosomes (HDs),<sup>1</sup> multiprotein complexes linking the epithelial intermediate fil-

ament network to the dermal anchoring fibrils (see Refs. 1 and 2 for review). HDs are formed by the clustering of several cytoplasmic and trans-membrane proteins (2). The cytoplasmic HD plaque components, which include HD1/plectin (3) and the bullous pemphigoid antigen 1 (BP230) (4), act as linkers for elements of the cytoskeleton at the cytoplasmic surface of plasma membrane. The trans-membrane constituents of HDs, which include the  $\alpha_6\beta_4$  integrin (5, 6) and the bullous pemphigoid antigen 2 (BP180) (7), serve as cell receptors connecting the cell interior to extracellular matrix proteins.

In particular, the  $\alpha_6\beta_4$  integrin is a receptor for the basement membrane component laminin-5, a heterotrimeric protein composed of three distinct polypeptides,  $\alpha 3$ ,  $\beta 3$ , and  $\gamma 2$ , which are encoded by three different genes known as *LAMA3*, *LAMB3*, and *LAMC2*, respectively (see Ref. 8 for review). Laminin-5 binds to the basal keratinocyte cell surface through the  $\alpha_6\beta_4$  integrin and tightens the dermal-epidermal junction by binding also to the N-terminal NC-1 domain of type VII collagen (9). The crucial importance of the interaction between laminin-5 and its  $\alpha_6\beta_4$  receptor in maintaining the integrity of the integument has been unambiguously proven by the generation of  $\alpha_6$ - and  $\beta_4$ -null mice (10–12) and by the identification of gene mutations in patients suffering from a devastating blistering disorder of the skin known as junctional epidermolysis bullosa (JEB). In most cases, JEB is due to mutations in *LAMA3*, *LAMB3*, and *LAMC2* genes (13–15) and in *ITGA6* and *ITGB4* genes, which encode  $\alpha_6$  and  $\beta_4$  integrin subunits, respectively (16, 17). Mutations in *ITGA6* and *ITGB4* are usually associated to pyloric atresia (PA)-JEB (16, 17).

The cytoplasmic domain of  $\alpha_6\beta_4$  contains two pairs of type III fibronectin (FN)-like repeats separated by a 142-amino acid connecting segment (CS). This CS is the target of multiple regulatory mechanisms, including tyrosine phosphorylation (18) and proteolytic processing (19). In particular, CS harbors tandem tyrosine phosphorylation sites (Tyr-1422 and Tyr-1440), which resemble the tyrosine activation motif (TAM) of immune receptors and are phosphorylated in response to the binding of  $\alpha_6\beta_4$  to laminin-5 (18). The potential TAM resides within a 303-amino acid segment of the  $\beta_4$  cytoplasmic domain that includes the first pair of type III FN-like repeats and the CS. Mutational studies have indicated that this segment of  $\beta_4$  is sufficient to mediate the incorporation of recombinant  $\beta_4$  into the existing HD-like adhesion of 804G cells (20). We initially observed that phenylalanine substitutions at either one of the two tyrosines in the potential TAM decreased the incorporation of recombinant  $\beta_4$  in HD-like adhesions (18). Although subsequent studies have yielded a contrasting result, they have

\*This work was supported by Telethon-Italy (Grants A.106 and B-53), by EEC BIOMED 2 N° Grant BMHG4-97-2062, and by Ministero della Sanità, Italy. The costs of publication of this article were defrayed in part by the payment of page charges. This article must therefore be hereby marked "advertisement" in accordance with 18 U.S.C. Section 1734 solely to indicate this fact.

|| To whom correspondence should be addressed: Laboratory of Tissue Engineering, I. D. I., Istituto Dermopatico dell'Immacolata, Via dei Castelli Romani, 83/85, 00040 Pomezia (Roma), Italy. Tel.: 39-06-9112192; Fax: 39-06-9106765; E-mail: m.deluca@idi.it.

<sup>1</sup> The abbreviations used are: HD, hemidesmosome; TAM, tyrosine activation motif; PA-JEB, pyloric atresia-junctional epidermolysis bullosa; CS, connecting segment; FN, fibronectin; mAb, monoclonal antibody.

provided evidence that the integrity of the TAM is required for efficient recruitment of BP180 by recombinant  $\beta_4$  in HD-like adhesions of PA-JEB keratinocytes (21, 22). We have recently obtained evidence that the original TAM mutant used by Mainiero *et al.* (18) was generated starting from a version of  $\beta_4$  that differs from the canonical form A because it lacks amino acids 941–948 (QDHTIVDT) in the membrane proximal portion of the cytoplasmic domain. The origin and nature of this variant form remain to be established. We have observed that this variant form of  $\beta_4$  and a canonical form carrying phenylalanine substitutions at Tyr-1422 or Tyr-1440 are both normally incorporated in the HD-like adhesions of 804G cells (23). However, a mutant  $\beta_4$  carrying both modifications is not, as shown previously (18).

In addition to resolving the prior controversy, these results reveal a functional synergy between amino acid stretches located relatively far apart in the linear sequence of the  $\beta_4$  cytoplasmic domain and highlight the necessity to further examine the potential role of the  $\beta_4$  TAM in HD assembly. Moreover, the potential role of specific portions of the  $\beta_4$  cytoplasmic domain, and in particular of the TAM, in interaction with other HD components and in HD assembly is based solely on the results obtained using immortalized cell lines cultured on plastic. Under these conditions, both keratinocytes and 804G cells do not form HDs. Instead, HD components (such as  $\alpha_6\beta_4$ , BP180, and HD1/plectin) are organized in typical patches in which spots correspond to microfilament-free areas (“leopard skin” pattern, as described in Ref. 24), often referred to as HD-like adhesions (22, 25).

This said, the functional role of HD components in the proper assembly of mature HDs can in fact be studied *in vitro* because normal human primary keratinocytes can be cultivated in conditions that allow full epithelial differentiation (26–28) and proper assembly of mature HDs (29, 30). Keratinocytes can generate cohesive sheets of stratified epithelium that maintains virtually the same differentiation features and gene expression pattern of its *in vivo* counterpart so that it can be routinely transplanted in patients suffering from large skin or mucosal defects (31–33). When primary keratinocytes are seeded onto dead de-epidermized dermis in organotypic cultures (29), mature HDs are formed *in vitro* (30). Therefore, the availability of human  $\beta_4$ -deficient primary keratinocytes (see “Results”), the possibility of stably transducing primary keratinocytes with high efficiency (34), and the possibility of subcultivating stably transduced cells in conditions in which HDs are formed (30) provide a unique opportunity to clarify the above uncertainties and to investigate the role of  $\beta_4$  and of its potential TAM in the formation of mature HDs.

#### EXPERIMENTAL PROCEDURES

**Cell Culture, cDNA Constructs, and Amphotropic Producer Cell Lines**—Swiss mouse 3T3-J2 cells (a gift from Howard Green, Harvard Medical School, Boston), GP+E-86 ecotropic packaging cells, and GP+env Am12 amphotropic packaging cells were grown as described (34). Normal human epidermal keratinocytes were obtained from skin biopsies of healthy volunteers. Primary  $\beta_4$ -null keratinocytes were obtained from a 1-cm<sup>2</sup> biopsy taken from a newborn patient suffering from PA-JEB (see “Results”). Informed consent was obtained from the parents. Keratinocytes were cultivated on a feeder layer of lethally irradiated 3T3-J2 cells as described (28, 30, 33) and passaged at the stage of subconfluence.

pRC/CMV- $\beta_4^{Y1422F}$ , pRC/CMV- $\beta_4^{Y1440F}$ , and pRC/CMV- $\beta_4^{Y1422F/Y1440F}$ , encoding  $\beta_4$  with phenylalanine substitutions in the TAM sequence, were constructed from partial cDNA clones covering the entire sequence of the canonical form A of  $\beta_4$  including the amino acid sequence QDHTIVDT (941–948) (35). A PCR fragment from pRC/CMV- $\beta_4$  restricted with *EcoRV* and *XhoI*, containing the 3' end of  $\beta_4$  (0.443 kilobase pairs), was inserted in pBS/SK to obtain pBS/SK3'end $\beta_4$ . A 4.968-kilobase pair fragment from pRC/CMV- $\beta_4$  restricted with *EcoRI* and *EcoRV* was inserted in pBS/SK3'end $\beta_4$  to obtain full-length pBS/

SK- $\beta_4$ . pLB4SN was constructed by cloning the 5.4-kilobase pair fragment from full-length pBS/SK- $\beta_4$  into the *EcoRI/XhoI* sites of pLXSN retroviral vector (36) as described previously (34). The other constructs were inserted into the *EcoRI/XhoI* sites of pLXSN retroviral vector as described above. All constructs were sequenced before the generation of producer cell lines.

Amphotropic producer cell lines carrying each of the above constructs were generated by the transinfection protocol as described (30, 34). A control amphotropic packaging cell line was generated as above using the pLXSN retroviral vector. For each producer cell line, the viral titer was higher than  $1 \times 10^5$  colony-forming units/ml.

**Retroviral-mediated Gene Transfer, *In Situ* Hybridization, and Southern and Northern Analysis**—Infection of primary keratinocytes was performed as described previously (30, 34). Briefly, subconfluent primary  $\beta_4$ -null keratinocytes were trypsinized and seeded ( $5 \times 10^3$  cells/cm<sup>2</sup>) onto a feeder layer ( $2.3 \times 10^4$  cells/cm<sup>2</sup>) composed of lethally irradiated 3T3-J2 cells and producer GP+env Am12 cells (a 1:2 mixture). After 3 days of cultivation, cells were collected and plated onto a regular 3T3-J2 feeder layer. Subconfluent cultures were used for further analysis.

Analysis of integrated proviral genomes was performed by Southern analysis as described (34). *In situ* hybridization was performed using the DIG Nucleic Acid Detection kit (Roche Molecular Biochemicals) following the manufacturer's instructions. Sections of cultured epidermal sheets were hybridized with a  $\beta_4$  integrin antisense riboprobe. For Northern analysis, cellular RNA was extracted with RNAfast (Sigma). 10  $\mu$ g of total RNA was size-fractionated through 1% agarose-formaldehyde gels and transferred to nylon membrane (Hybond N<sup>+</sup>, Amersham Pharmacia Biotech). Blots were prehybridized at 68 °C for 2 h in 50% formamide, 5 $\times$  SSC, 0.02% SDS, 2% blocking reagent, and 0.1% N-laurylsarcosine. Hybridization was performed overnight in the same conditions with the addition of <sup>32</sup>P-labeled  $\beta_4$  integrin fragment *SacII* (335)/*HindIII* (1129) probes ( $2 \times 10^6$  cpm/ml). Filters were washed at high stringency in standard conditions.

**Immunological Analysis**—The following antibodies were used: mouse 3E1 mAb, raised against the extracellular domain of  $\beta_4$  (Life Technologies, Inc.); goat (N20, Santa Cruz Biotechnology, Santa Cruz, CA) and rabbit polyclonal antiserum (37), both reacting against the  $\beta_4$  N terminus; rat G0H3 mAb (Serotec) and goat polyclonal T20 (Santa Cruz Biotechnology), recognizing the  $\alpha_6$  integrin; and HD121 and 1D1 mAbs (gift from Dr. K. Owaribe, Nagoya University, Nagoya, Japan) recognizing HD1/plectin and BP180, respectively.

Immunofluorescence and immunohistochemistry were performed as described (28, 30, 38). For immunoblotting, subconfluent keratinocytes were extracted on ice with lysis radioimmune precipitation buffer (50 mM Tris/HCl, pH 8.5, 150 mM NaCl, 1% deoxycholate, 1% Triton X-100, 0.1% SDS, 0.2% sodium azide). Protein content was determined by the BCA assay (Pierce). Equal amounts of total proteins were immunoprecipitated with an excess of antibody, separated by SDS-PAGE, and transferred to a nitrocellulose filter. The blot was incubated in TBST (10 mM Tris-HCl, pH 8.0, 150 mM NaCl, and 0.05% Tween 20) containing 1% bovine serum albumin, washed, and probed with specific antibodies for 1 h at room temperature. Nitrocellulose-bound antibodies were detected by chemiluminescence with ECL (Amersham Pharmacia Biotech).

Immunoprecipitations were carried out on surface-radiolabeled keratinocytes as described (39). Briefly, subconfluent keratinocytes were detached with 10 mM EDTA in phosphate-buffered saline (PBS), pH 7.4, and then washed and resuspended in PBS ( $2 \times 10^7$  cells/ml). Iodination was carried out for 15 min at room temperature in the presence of 1 mCi/ml of [<sup>125</sup>I]iodine (Amersham Pharmacia Biotech), 0.6 mg of lactoperoxidase, and 0.003% H<sub>2</sub>O<sub>2</sub>. After washing with 5 mM KI in PBS, cells were lysed in radioimmune precipitation buffer, pH 8.5, containing protease inhibitors (Complete<sup>TM</sup>, Roche Molecular Biochemicals). Immunoprecipitations were carried out by overnight incubation at +4 °C of the immunoabsorbents (antibodies adsorbed onto Protein A-Sepharose, Amersham Pharmacia Biotech) with samples of cell lysates followed by extensive washing and elution by boiling in Laemmli sample buffer. Samples were then analyzed by SDS-PAGE under nonreducing conditions on 6% polyacrylamide gels followed by autoradiography. Protein-bound radioactivity in cell lysates was counted, and equivalent amounts of radioactivity were immunoprecipitated for each sample.

**Organotypic Cultures and Transmission Electron Microscopy**—Keratinocytes ( $5 \times 10^4$  cells/cm<sup>2</sup>) were seeded onto dead de-epidermized dermis and cultivated as described (30). 7 days later, cultures were lifted at the air-liquid interface, cultured for 1 additional week, and then processed for electron microscopy. Briefly, specimens were fixed in 2% glutaraldehyde, post-fixed in 1% osmium tetroxide, dehydrated in



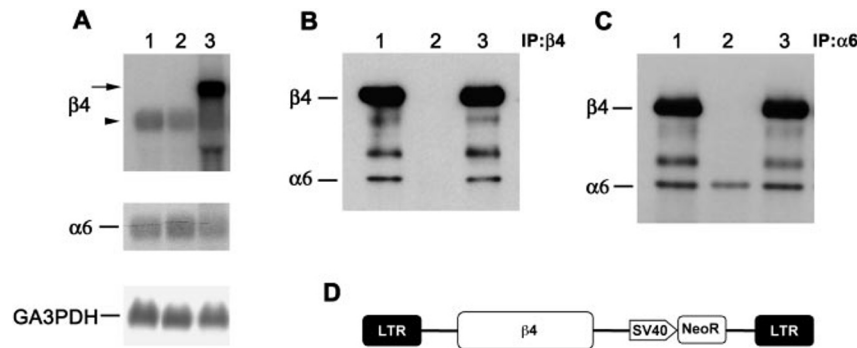


FIG. 1. *A*, Northern analysis. 10  $\mu$ g of total RNA obtained from control (1),  $\beta_4$ -null (2), and  $\beta_4$ -corrected (3) keratinocytes was separated by electrophoresis, transferred to nylon filters, and hybridized to a  $^{32}$ P-labeled  $\beta_4$ -probe, to a  $^{32}$ P-labeled  $\alpha_6$  probe, or to a  $^{32}$ P-labeled GA $_3$ PDH probe. Exogenous (arrow) and endogenous (arrowhead)  $\beta_4$  transcripts are indicated. The molecular weight differences in the ectopic versus endogenous message are explained by the presence of the SV40 early promoter (SV40) and the neomycin resistance gene (NeoR) in the retroviral construct (panel D). *B* and *C*, immunoprecipitation and Western analysis. Cell extracts were prepared from control (1),  $\beta_4$ -null (2), and  $\beta_4$ -corrected (3) keratinocytes. Equal amounts of cell lysates were immunoprecipitated using mAbs to either  $\beta_4$  (*B*, IP: $\beta_4$ ) or  $\alpha_6$  (*C*, IP: $\alpha_6$ ) (3E1 and G0H3, respectively). Eluates were fractionated on 7.5% SDS-polyacrylamide gel, transferred to nitrocellulose filters, and immunostained with antisera raised against  $\alpha_6$  (T20) and  $\beta_4$  (N20), respectively. *D*, schematic map of the pLB4SN provirus. Solid boxes indicate the viral long terminal repeat (LTR), open boxes indicate the full-length  $\beta_4$  ( $\beta_4$ ) and neomycin phosphotransferase (NeoR) cDNAs, and the arrowhead-shaped box indicates the simian virus 40 early promoter.

graded alcohols, embedded in Epon resin, and sectioned on an ultramicrotome (Reichert Ultracut E, Leica, Wien, Austria). Ultrathin sections were stained with uranyl acetate and lead citrate and observed with a transmission electron microscope (CM100, Philips, Eindhoven, The Netherlands). Organotypic cultures were also sectioned on a cryostat and then analyzed by immunofluorescence as described (30).

**Morphometry**—Electron micrographs of overlapping fields of the dermal-epidermal junction, taken at a magnification of  $\times \sim 15,500$ , were printed and assembled into a montage with a final magnification of  $\times 40,000$ . The prints were digitalized, using a scanner (HP ScanJet 4c), in bitmap format, and the files were analyzed using a semi-automatic image analysis system (Kontron Elektronik Imaging System KS 300). The length of dermal-epidermal junction was measured for each point, commencing at one end of the montage, and the number of HDs was counted. For each HD, the area was measured, and the percentage of HDs associated with tonofilaments was calculated. A total of 1,291  $\mu$ m of cell membrane was examined, divided into: 162  $\mu$ m for control keratinocytes, 116  $\mu$ m for  $\beta_4$ -null keratinocytes, 116  $\mu$ m for  $\beta_4$ -corrected keratinocytes, and 244, 441, and 212  $\mu$ m for  $\beta_4^{Y1422F}$ ,  $\beta_4^{Y1440F}$ , and  $\beta_4^{Y1422F/Y1440F}$  keratinocytes, respectively. A total of 443 HDs were examined, divided into: 150 for control keratinocytes, 0 for  $\beta_4$ -null keratinocytes, 106 for  $\beta_4$ -corrected keratinocytes, and 27, 130, and 30 for  $\beta_4^{Y1422F}$ ,  $\beta_4^{Y1440F}$ , and  $\beta_4^{Y1422F/Y1440F}$  keratinocytes, respectively.

## RESULTS

Keratinocytes were cultivated from a 1-cm $^2$  skin biopsy taken from a newborn patient presenting with the clinical hallmarks of PA-JEB. The proband was a compound heterozygote for a 3-base pair deletion ( $\Delta$ N318) in exon 8 of the maternal allele of the *ITGB4* gene and an as yet unidentified paternal genetic defect. Allele-specific amplification of transcripts did not show any mRNA deriving from the paternal mutant allele, even in cycloheximide-treated cells.<sup>2</sup> Immunohistochemical analysis showed absence of the  $\beta_4$  integrin in the skin of the proband (not shown). The keratinocytes of the proband are hereafter referred to as  $\beta_4$ -null keratinocytes.

Northern blot analysis (Fig. 1) and *in situ* hybridization performed on cultured epidermal sheets (Fig. 2) showed similar levels of  $\beta_4$  transcripts in  $\beta_4$ -null keratinocytes (Fig. 1A, lane 2, arrowhead, and Fig. 2C) as compared with normal control cells (Fig. 1A, lane 1, arrowhead, and Fig. 2A). Absence of the  $\beta_4$  polypeptide in  $\beta_4$ -null cells was confirmed by immunoprecipitation followed by Western blot analysis (Fig. 1, B and C, lanes 2), immunofluorescence performed on  $\beta_4$ -null colonies (not shown), and immunohistochemistry performed on cultured epi-

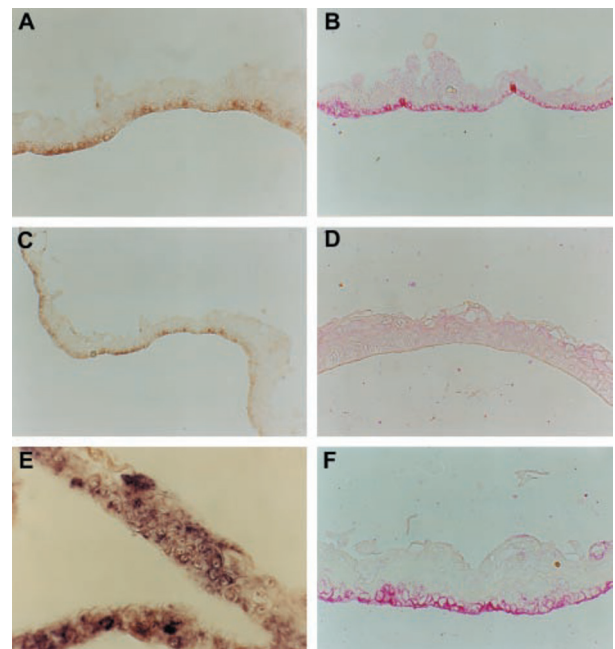


FIG. 2. *In situ* hybridization and immunohistochemistry. Cultured epidermal sheets were prepared from primary cultures of control (A and B),  $\beta_4$ -null (C and D), and  $\beta_4$ -corrected keratinocytes (E and F). Sections of cultured epidermal sheets were either hybridized with a  $\beta_4$  integrin antisense riboprobe (A, C, and E) or immunostained with a rabbit antiserum raised against  $\beta_4$  (B, D, and F) (19).

dermal sheets generated by  $\beta_4$ -null keratinocytes (Fig. 2D). Thus, although transcription of mutated  $\beta_4$  can occur in  $\beta_4$ -null cells, the  $\beta_4$  polypeptide is either not translated or is rapidly degraded. The  $\alpha_6$  subunit (Fig. 1C, lane 2) was expressed at levels comparable with those observed in control cells (Fig. 1C, lane 1).

**Gene Correction of  $\beta_4$ -null Primary Keratinocytes**—Subconfluent primary cultures of  $\beta_4$ -null keratinocytes were used for experiments aimed at corrective  $\beta_4$  gene transfer. Infections with replication-defective retroviruses carrying a full-length human  $\beta_4$  cDNA (Fig. 1D) were performed by co-culturing  $\beta_4$ -null keratinocytes with lethally irradiated 3T3-J2 cells and producer GP+envAm12 cells (30, 38). Keratinocytes were then transferred onto a regular 3T3-J2 feeder layer both at regular density ( $5 \times 10^3$ /cm $^2$ ) and at clonal density (100–1,000 cells/

<sup>2</sup> Zambruno, G., unpublished data.

dish) so that each colony was formed by a single cell and could be scored as  $\beta_4^+$  and  $\beta_4^-$ .

Southern analysis showed multiple bands resulting from numerous proviral integrations in a heterogeneous transduced cell population (not shown, see also Ref. 34). Accordingly, Northern analysis showed abundant levels of exogenous  $\beta_4$  transcripts (Fig. 1A, lane 3, arrow). Immunofluorescence (performed on coverslips seeded with keratinocytes plated at clonal density) demonstrated that clonogenic  $\beta_4$ -null keratinocytes were transduced with an efficiency of virtually 100% and that the exogenous  $\beta_4$  polypeptide was localized at the cell membrane (not shown). The proper assembly of the  $\alpha_6\beta_4$  heterodimer was evidenced by immunoprecipitation of cell lysates using mAbs to either  $\beta_4$  or  $\alpha_6$  (3E1 and G0H3, respectively) followed by immunoblot using antisera raised against either  $\alpha_6$  or  $\beta_4$  (T20 and N20, respectively). As shown in Fig. 1 (panels B and C),  $\alpha_6\beta_4$ , which was absent in  $\beta_4$ -null cells (lane 2), was readily detected in  $\beta_4$ -transduced keratinocytes (lanes 3) at levels comparable with those detected in normal control cells (lane 1). *In situ* hybridization (performed on epithelial sheets generated by  $\beta_4$ -transduced keratinocytes) showed abundant levels of exogenous  $\beta_4$  transcripts both in basal and suprabasal  $\beta_4$ -corrected cells (Fig. 2E). The suprabasal expression of exogenous  $\beta_4$  transcripts is expected because expression of the transgene is driven by the retroviral long terminal repeat. However, immunohistochemical analysis revealed that both in normal control cells (Fig. 2B) and in  $\beta_4$ -corrected keratinocytes (Fig. 2F), the expression of the  $\beta_4$  polypeptide was restricted to the basal layer of cultured epidermal sheets. It is possible that, in the absence of its natural  $\alpha_6$  partner, exogenous  $\beta_4$  is rapidly degraded in the ER of suprabasal layers.

The localization of  $\alpha_6\beta_4$  and of other HD components was then investigated in organotypic cultures, namely in conditions allowing the formation of mature HDs. In normal control cultures,  $\alpha_6\beta_4$  was clearly concentrated at the basal pole of basal keratinocytes (Fig. 3A). As described previously (40), in wound healing and in organotypic cultures, a faint labeling of the lateral and apical surfaces of the basal and first suprabasal cell layer was observed (Fig. 3A). The dermal-epidermal junction was also blotted by anti-HD1/plectin (Fig. 3B) and anti-BP180 (not shown) mAbs. In  $\beta_4$ -null organotypic cultures,  $\beta_4$  was virtually undetectable (Fig. 3C), whereas the  $\alpha_6$  subunit was not polarized and was diffusely distributed in the basal keratinocyte cytoplasm (not shown). Similarly, HD1/plectin (Fig. 3D) and BP180 (not shown) were not concentrated at the dermal-epidermal junction but were diffusely distributed in the cytoplasm of basal keratinocytes. Gene correction of  $\beta_4$ -null keratinocytes restored the normal expression pattern of  $\beta_4$  (Fig. 3E), HD1/plectin (Fig. 3F), and BP180 (not shown). Indeed, the level of expression and the localization at the dermal-epidermal junction of the polypeptides were very similar to those observed in normal control cells (Fig. 3, A and B).

The formation of mature HDs was investigated by transmission electron microscopy performed on ultrathin sections of organotypic skin cultures. As shown in Fig. 4, normal control keratinocytes (A) and  $\beta_4$ -corrected keratinocytes (B) assembled mature HDs (stars), displaying clearly recognizable sub-basal dense plates and cytoplasmic outer and inner plaques associated with keratin intermediate filaments (arrows) distributed along their basal plasma membrane. In contrast, very few rudimentary HDs, which appeared as small, moderately electron-dense spots almost completely lacking a tripartite structure and association with keratin filaments, could be identified in  $\beta_4$ -null keratinocytes (F). Thus,  $\beta_4$ -corrected keratinocytes were almost indistinguishable from normal control cells in terms of  $\alpha_6\beta_4$  expression, the localization of HD components,

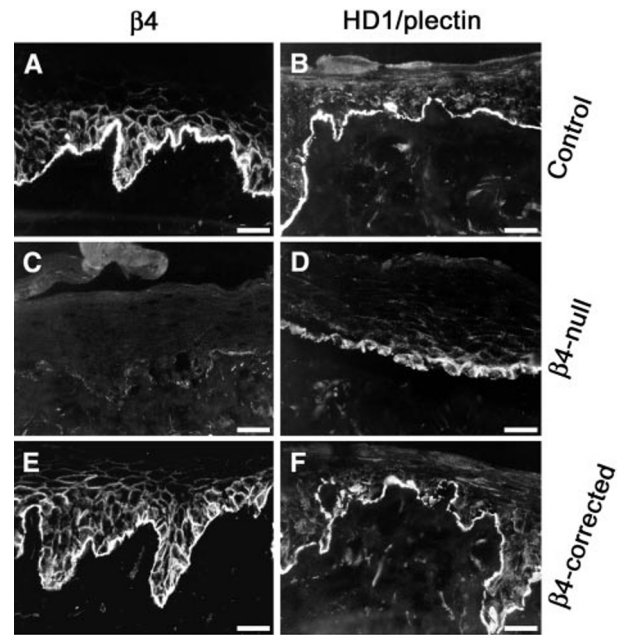


FIG. 3. Immunofluorescence analysis of HD components in organotypic skin cultures. A and B, normal control keratinocytes. C and D,  $\beta_4$ -null keratinocytes. E and F,  $\beta_4$ -corrected cells. Sections of organotypic cultures were stained with an anti- $\beta_4$  mAb (A, C, and E) and with an anti-HD1/plectin mAb (B, D, and F). Note that in control cells and in  $\beta_4$ -corrected keratinocytes,  $\beta_4$  and HD1/plectin were concentrated at the basal pole of basal keratinocytes, clearly delimiting the dermal-epidermal junction. In contrast, in  $\beta_4$ -null cells,  $\beta_4$  was undetectable and HD1/plectin staining was mostly pericellular.

and HD structure and density, suggesting that the adhesive properties of  $\beta_4$ -null keratinocytes were fully restored.

**Expression of  $\beta_4$  Mutants in Primary  $\beta_4$ -null Keratinocytes**—To investigate the role of  $\beta_4$  TAM in HD formation and maturation, subconfluent primary cultures of  $\beta_4$ -null keratinocytes were stably transduced with replication-defective retroviruses carrying cDNA(s) encoding: (i)  $\beta_4$  with a phenylalanine substitution at Tyr-1422 ( $\beta_4^{Y1422F}$ ), (ii)  $\beta_4$  with a phenylalanine substitution at Tyr-1440 ( $\beta_4^{Y1440F}$ ), and (iii)  $\beta_4$  with a combined replacement of Tyr-1422 and Tyr-1440 ( $\beta_4^{Y1422F/Y1440F}$ ) (Fig. 5A). Proviral integration was demonstrated by Southern hybridization (not shown). As shown in Fig. 5B, variable levels of the different  $\beta_4$  transcripts were detected in transduced  $\beta_4$ -null keratinocytes (arrow).

The assembly of the  $\alpha_6\beta_4$  heterodimer in cells transduced with different mutants was investigated by immunoprecipitation of cell lysates using anti- $\beta_4$  mAbs (3E1) followed by immunoblot using antisera raised against either  $\alpha_6$  or  $\beta_4$  (T20 and N20, respectively). As shown in Fig. 5C, all mutants were able to associate to the  $\alpha_6$  subunit (lanes 2–4). It is worth noting that comparable amounts of the  $\alpha_6\beta_4$  heterodimer were expressed in all transduced keratinocytes (Fig. 5C).

The exposure of  $\beta_4$  on the keratinocyte plasma membrane was evaluated by immunoprecipitation of cell lysates prepared from surface-radioiodinated cells, using the anti- $\beta_4$  3E1 mAb. As shown in Fig. 5D, equal amounts of  $\beta_4$  were exposed on the cell surface in normal control cells (lane 1),  $\beta_4$ -corrected cells (lane 2), and  $\beta_4$ -null cells transduced with different TAM mutants ( $\beta_4^{Y1422F}$ ,  $\beta_4^{Y1440F}$ ,  $\beta_4^{Y1422F/Y1440F}$ , lanes 3, 4, and 5, respectively). These data suggest that the  $\beta_4$  TAM is not essential for the localization of the  $\alpha_6\beta_4$  integrin at the keratinocyte plasma membrane.

**The Role of  $\beta_4$  TAM Domains in HD Formation and Maturation**—The localization of  $\beta_4$  mutants and of other HD components as well as the formation of mature HDs were investi-



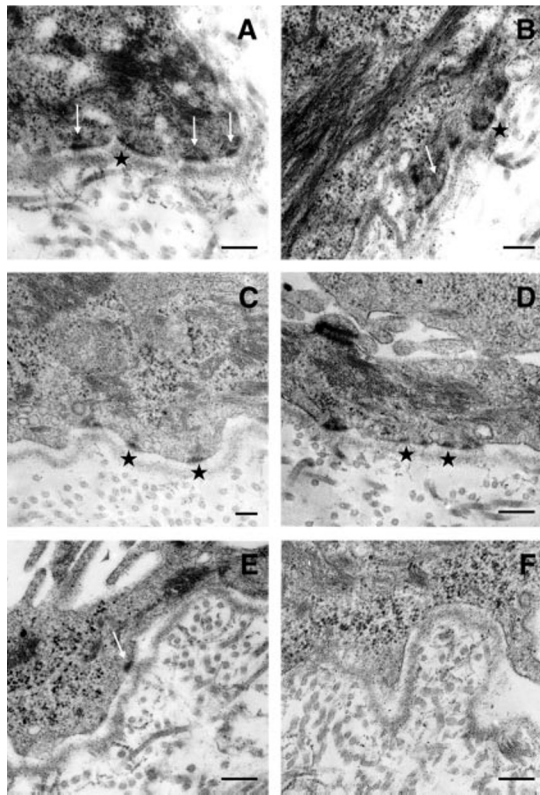


**FIG. 4. Transmission electron microscopy.** Ultrastructural examination of the dermal-epidermal junction of organotypic skin cultures showed that, similarly to normal control keratinocytes (A),  $\beta_4$ -corrected keratinocytes (B) assemble mature HDs displaying sub-basal dense plates (stars) and outer and inner cytoplasmic plaques associated with bundles of keratin intermediate filaments (arrows). (Anchoring filaments transverse the lamina lucida are also visible, more frequently below the HD.)  $\beta_4^{Y1422F}$  (C) and  $\beta_4^{Y1440F}$  (D) keratinocytes also display HDs (stars), which appear, however, less numerous and smaller with reduction in keratin filament association. More severe HD alterations typify  $\beta_4^{Y1422F/Y1440F}$  keratinocytes (E, at arrow), in which sub-basal dense plates appear greatly attenuated and cytoplasmic inner plaques and keratin filament insertion are almost undetectable. A marked decrease in anchoring filament density is also evident in  $\beta_4$ -null and  $\beta_4^{Y1422F/Y1440F}$  keratinocytes. Bar, 200 nm.

gated by immunofluorescence and transmission electron-microscopy performed on ultrathin sections of organotypic skin cultures. Immunofluorescence analysis performed on organotypic cultures prepared from  $\beta_4^{Y1422F}$  (Fig. 6, A and B),  $\beta_4^{Y1440F}$  (Fig. 6, C and D), and  $\beta_4^{Y1422F/Y1440F}$  (Fig. 6, E and F) keratinocytes showed that  $\beta_4$  mutants (Fig. 6, A, C, and E) and HD1/plectin (Fig. 6, B, D, and F) as well as  $\alpha_6$  integrin and BP180 (not shown) were not properly concentrated at the dermal-epidermal junction. Indeed,  $\beta_4$  and HD1/plectin (as well as  $\alpha_6$  and BP180) staining was clearly pericellular and of variable intensity in most areas. This is in sharp contrast with normal control cells (Fig. 3, A and B) and  $\beta_4$ -corrected cells (Fig. 3, E and F) in which  $\beta_4$  (Fig. 3, A and E) and HD1/plectin (Fig. 3, B and F) as well as  $\alpha_6$  and BP180 (not shown) were concentrated at the basal pole of basal keratinocytes, clearly delimiting the dermal-epidermal junction. It is worth noting that  $\beta_4$  and HD1/plectin appeared occasionally polarized in some basal  $\beta_4^{Y1422F}$  (Fig. 6, A and B, arrow) and  $\beta_4^{Y1440F}$  (Fig. 6, C and D, arrows) cells, whereas a virtually complete impairment of  $\beta_4$  and HD1/plectin polarization was evident in  $\beta_4^{Y1422F/Y1440F}$  keratinocytes (Fig. 6, E and F).

As shown in Fig. 4, while  $\beta_4$ -null keratinocytes (F) displayed very rare rudimentary HDs,  $\beta_4$ -corrected keratinocytes (B) as well as  $\beta_4^{Y1422F}$  (C),  $\beta_4^{Y1440F}$  (D), and  $\beta_4^{Y1422F/Y1440F}$  (E) cells were able to form HDs, although with striking morphological and

numerical differences. While HD structure and density in  $\beta_4$ -corrected keratinocytes (B) were virtually indistinguishable from normal control cells (A), a reduction in HD number, size, tripartite structure definition, and keratin filament association was evident in  $\beta_4^{Y1422F}$  (C),  $\beta_4^{Y1440F}$  (D), and  $\beta_4^{Y1422F/Y1440F}$  (E) cells. Indeed, rare HD-like structures almost completely lacking sub-basal dense plates were detected in  $\beta_4^{Y1422F/Y1440F}$  cells (E). In most of these structures, the inner cytoplasmic plaque as well as keratin filaments that insert on cytoplasmic electron-dense plaques were almost undetectable. A marked decrease in anchoring filament density was evident in  $\beta_4$ -null (F) and  $\beta_4^{Y1422F/Y1440F}$  (E) keratinocytes.

To quantify the number of HDs, the level of their maturation, and the extent of their association to intermediate filaments, a morphometric analysis of the dermal-epidermal junction was undertaken on electron micrographs of overlapping fields (41) (see "Experimental Procedures"). We have analyzed 1,291  $\mu\text{m}$  of basal membrane and 443 HDs (see Table I and "Experimental Procedures"). All measurements were made by the same observer at least three times on randomly selected montages. Measurements were made on montages obtained from two different experiments, and average values are indicated.

As shown in Table I, we did not detect mature HDs in  $\beta_4$ -null keratinocytes, whereas the mean values for HD counts in control cells (9.3 HDs/10  $\mu\text{m}$ ) and  $\beta_4$ -corrected keratinocytes (9.1 HDs/10  $\mu\text{m}$ ) were similar. In contrast, the number of detectable HDs was strikingly reduced (up to 8-fold) in  $\beta_4^{Y1422F}$  (1.1 HDs/10  $\mu\text{m}$ ),  $\beta_4^{Y1440F}$  (2.9 HDs/10  $\mu\text{m}$ ), and  $\beta_4^{Y1422F/Y1440F}$  (1.6 HDs/10  $\mu\text{m}$ ) keratinocytes. Statistical analysis of the size of HDs was calculated using KS 300, a semiautomatic image analysis system, and data fell into a Gaussian distribution. The average size of HDs of control (3,897  $\text{nm}^2$ ) and  $\beta_4$ -corrected (3,366  $\text{nm}^2$ ) keratinocytes was similar. Phenylalanine substitution at tyrosine 1422 and 1440 determined a reduction of HD size (2692  $\text{nm}^2$  and 2181  $\text{nm}^2$ , respectively). Analysis of keratin filament association showed a marked reduction of the ability of  $\beta_4^{Y1440F}$  and  $\beta_4^{Y1422F/Y1440F}$  HDs to associate to intermediate filaments as compared with control and  $\beta_4$ -corrected cells (Table I). It is worth noting, however, that even if the number of HDs formed by  $\beta_4^{Y1422F}$  keratinocytes was dramatically reduced, their ability to associate to intermediate filaments was only slightly altered. Taken together, these data indicate that  $\beta_4$  TAMs are essential for the formation of a correct number of mature HDs in basal keratinocytes.

## DISCUSSION

The requirement for the cytoplasmic domain of  $\beta_4$  integrin in HD assembly has been clearly documented (42), and the results of this study indicate that the integrity of both tyrosine 1422 and 1440 of the  $\beta_4$  cytoplasmic TAM is demanded for the optimal assembly of *bona fide* HDs in human epidermis. This conclusion stands in clear contrast to prior studies indicating that TAM-mutant  $\beta_4$  localizes efficiently to endogenous HD-like adhesions of 804G cells and that it promotes assembly of HD-like adhesions in (immortalized) PA-JEB keratinocytes (22, 23), thus indicated that  $\beta_4$  TAM is dispensable for HD formation (22).

It is likely that the assembly of mature HDs has more complex molecular requirements than the formation of HD-like adhesions, which reflect the co-localization of HD components at the basal pole of cells cultivated on plastic (24). For instance, it has been suggested that the first pair of type III FN-like modules and the initial segment of the CS of  $\beta_4$  interact directly with the actin binding domain of HD1/plectin (21, 43, 44), whereas the cytoplasmic N terminus of BP180 associates with BP230 (45). In turn, HD1/plectin and BP230 associate with keratin filaments (46). Thus, both  $\alpha_6\beta_4$  and BP180 can interact

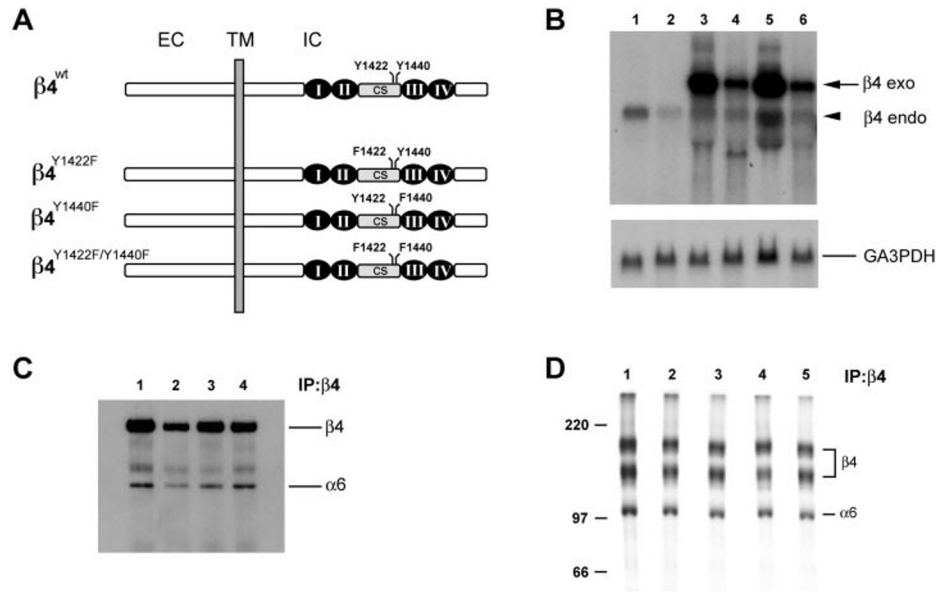


FIG. 5. A, schematic map of the different  $\beta_4$  isoforms used to transduce  $\beta_4$ -null keratinocytes. EC, TM, and IC indicate extracellular, transmembrane, and cytoplasmic domain, respectively. Amino acid substitutions in the CS segment are indicated. Black circles indicate the FN-like repeats. B, Northern analysis. 10  $\mu$ g of total RNA obtained from control (1),  $\beta_4$ -null (2),  $\beta_4$ -corrected (3),  $\beta_4^{Y1422F}$  (4),  $\beta_4^{Y1440F}$  (5), and  $\beta_4^{Y1422F/Y1440F}$  (6) keratinocytes was separated by electrophoresis, transferred to nylon filters, and hybridized to a  $^{32}$ P-labeled  $\beta_4$ -probe or to a  $^{32}$ P-labeled GA $_3$ PDH probe. C, immunoprecipitation and Western analysis. Cell extracts were prepared from  $\beta_4$ -corrected (1),  $\beta_4^{Y1422F}$  (2),  $\beta_4^{Y1440F}$  (3), and  $\beta_4^{Y1422F/Y1440F}$  (4) keratinocytes. Equal amounts of cell lysates were immunoprecipitated using anti- $\beta_4$  3E1 mAbs (IP: $\beta_4$ ). Eluates were then fractionated on 7.5% SDS-polyacrylamide gel, transferred to nitrocellulose filters, and immunostained with antisera raised against  $\alpha_6$  and  $\beta_4$  (T20 and N20, respectively). D, immunoprecipitation. Cell extracts were prepared from surface-radioiodinated normal control cells (1),  $\beta_4$ -corrected cells (2),  $\beta_4^{Y1422F}$  (3),  $\beta_4^{Y1440F}$  (4), and  $\beta_4^{Y1422F/Y1440F}$  (5) keratinocytes. Equal amounts of cell lysates were immunoprecipitated using anti- $\beta_4$  3E1 mAbs (IP: $\beta_4$ ). Eluates were then fractionated on 7.5% SDS-polyacrylamide gel and autoradiographed.

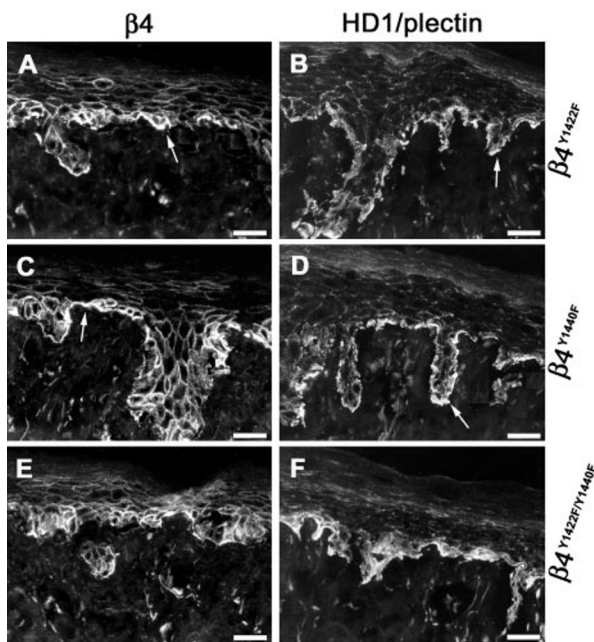


FIG. 6. Immunofluorescence analysis of HD components in organotypic skin cultures. A and B,  $\beta_4^{Y1422F}$  cells. C and D,  $\beta_4^{Y1440F}$  cells. E and F,  $\beta_4^{Y1422F/Y1440F}$  cells. Sections of organotypic cultures were stained with an anti- $\beta_4$  mAb (A, C, and E) and with an anti-HD1/plectin mAb (B, D, and F). Note that  $\beta_4$  and HD1/plectin staining was mostly pericellular in cells transduced with  $\beta_4$  mutants.  $\beta_4$  and HD1/plectin appeared occasionally polarized in some basal  $\beta_4^{Y1422F}$  and  $\beta_4^{Y1440F}$  cells but very rarely in  $\beta_4^{Y1422F/Y1440F}$  keratinocytes (arrows in panels A–F). Thus, the cellular distribution of HD1/plectin was very similar in  $\beta_4$ -null cells (Fig. 3, panel D) and in  $\beta_4^{Y1422F/Y1440F}$  keratinocytes (panel F).

independently of each other with the keratinocyte intermediate filaments. Moreover, because the CS distal segment and the third type III FN-like module of  $\beta_4$  associate with the cytoplasmic domain of BP180 (22), it is likely that  $\alpha_6\beta_4$  and BP180

TABLE I  
Morphometric analysis

Cell strain	$\mu$ m of cell membrane analyzed	N° HDs analyzed	N° of HD/10 $\mu$ m of cell membrane	HD-presenting tonofilaments
controls	162	150	9.3	51%
$\beta_4$ -null	116	12 <sup>a</sup>	1.0 <sup>a</sup>	0%
$\beta_4$ -corrected	116	106	9.1	42%
$\beta_4^{Y1422F}$	244	27	1.1	39%
$\beta_4^{Y1440F}$	441	130	2.9	19%
$\beta_4^{Y1422F/Y1440F}$	212	35 <sup>a</sup>	1.7 <sup>a</sup>	18%

<sup>a</sup> Rudimentary HDs appearing as small or elongated electron-dense areas.

interact as a functional unit with the two plakins and thereby with the keratin cytoskeleton.

This said, mature HDs are formed *in vitro* only when keratinocytes are cultivated onto de-epidermized dermis (29, 30), as in the organotypic cultures shown here. This suggests that HD-like adhesions do not recapitulate the assembly of mature HDs and might explain discrepancies between our data and data reported previously (22).

What is the mechanism by which the two tyrosine residues of the potential  $\beta_4$  TAM regulate HD assembly? The immune receptor TAMs interact in a phosphorylation-dependent manner with the tandem SH2 domains of downstream target effectors, such as the protein kinase Syk and ZAP70 (47). Based on this observation, we have previously hypothesized that phosphorylation of the potential  $\beta_4$  TAM might activate a signaling pathway necessary for proper HD formation (18). Two lines of evidence suggest that this hypothesis has to be re-evaluated. First, phosphorylation of Tyr-1422 and Tyr-1440 in response to activation of the EGF receptor correlates with disassembly (not increased assembly) of HDs (37). Second, we have recently observed that exposure to the tyrosine phosphatase inhibitor, pervanadate, promotes tyrosine phosphorylation of  $\beta_4$  and disrupts HDs. Interestingly, this effect is largely suppressed by

phenylalanine substitutions at Tyr-1422 and Tyr-1440 (23). These more recent findings suggest the alternative hypothesis that the hydroxyl groups of Tyr-1422 and Tyr-1440 may be necessary for interaction with HD components such as, for instance, BP180 (22). In this model, phosphorylation of the two tyrosines may have a similar or even larger effect than their substitution to phenylalanine. Finally, there is evidence suggesting that the C-terminal tail of  $\beta_4$  folds and binds intramolecularly to a 321 amino acid segment that includes the first pair of type III FN-like repeats and part of the CS (22, 43). Since it has been speculated that this intramolecular bond may have to be disrupted to allow for association of  $\beta_4$  with HD1/ plectin and/or BP180, it is possible that substitutions of the two tyrosines with phenylalanine interfere with this postulated conformational change. Future studies will distinguish among these possibilities.

**Acknowledgments**—We thank Anna Bucci, Massimo Teson, and Daniela D'Agostino for technical help. We also thank the art department of Istituto Dermopatico dell'Immacolata for the artwork.

## REFERENCES

- Christiano, A. M., and Uitto, J. (1996) *Exp. Dermatol.* **5**, 1–11
- Borradori, L., and Sonnenberg, A. (1999) *J. Invest. Dermatol.* **112**, 411–418
- Wiche, G. (1998) *J. Cell Sci.* **111**, 2477–2486
- Stanley, J. R., Hawley-Nelson, P., Yuspa, S. H., Shevach, E. M., and Katz, S. I. (1991) *Cell* **64**, 897–903
- De Luca, M., Tamura, R. N., Kajiji, S., Bondanza, S., Rossino, P., Cancedda, R., Marchisio, P. C., and Quaranta, V. (1990) *Proc. Natl. Acad. Sci. U. S. A.* **87**, 6888–6892
- Stepp, M. A., Spurr-Michaud, S., Tisdale, A., Elwell, J., and Gibson, I. K. (1990) *Proc. Natl. Acad. Sci. U. S. A.* **87**, 8970–8974
- Giudice, G. J., Emery, D. J., and Diaz, L. A. (1992) *J. Invest. Dermatol.* **99**, 243–250
- Aumailley, M., and Krieg, T. (1996) *J. Invest. Dermatol.* **106**, 209–214
- Rousselle, P., Keene, D. R., Ruggiero, F., Champiaud, M. F., van der Rest, M., and Burgeson, R. E. (1997) *J. Cell Biol.* **138**, 719–728
- Dowling, J., Yu, Q. C., and Fuchs, E. (1996) *J. Cell Biol.* **134**, 559–572
- Georges-Labouesse, E., Messaddeq, N., Yehia, G., Cadalbert, L., Dierich, A., and Le Meur, M. (1996) *Nat. Genet.* **13**, 370–373
- van der Neut, R., Krimpenfort, P., Calafat, J., Niessen, C. M., and Sonnenberg, A. (1996) *Nat. Genet.* **13**, 366–369
- Aberdam, D., Galliano, M. F., Vailly, J., Pulkkinen, L., Bonifas, J., Christiano, A. M., Tryggvason, K., Uitto, J., Epstein, E.-H., Ortonne, J. P., and Meneguzzi, G. (1994) *Nat. Genet.* **6**, 299–304
- Pulkkinen, L., Christiano, A. M., Gerecke, D., Wagman, D. W., Burgeson, R. E., Pittelkow, M. R., and Uitto, J. (1994) *Genomics* **24**, 357–360
- Vidal, F., Baudoin, C., Miquel, C., Galliano, M. F., Christiano, A. M., Uitto, J., Ortonne, J. P., and Meneguzzi, G. (1995) *Genomics* **30**, 273–280
- Vidal, F., Aberdam, D., Miquel, C., Christiano, A. M., Pulkkinen, L., Uitto, J., Ortonne, J. P., and Meneguzzi, G. (1995) *Nat. Genet.* **10**, 229–234
- Ruzzi, L., Gagnoux-Palacios, L., Pinola, M., Belli, S., Meneguzzi, G., D'Alessio, M., and Zambruno, G. (1997) *J. Clin. Invest.* **99**, 2826–2831
- Mainiero, F., Pepe, A., Wary, K. K., Spinardi, L., Mohammadi, M., Schlessinger, J., and Giancotti, F. G. (1995) *EMBO J.* **14**, 4470–4481
- Giancotti, F. G., Stepp, M. A., Suzuki, S., Engvall, E., and Ruoslahti, E. (1992) *J. Cell Biol.* **118**, 951–959
- Spinardi, L., Ren, Y. L., Sanders, R., and Giancotti, F. G. (1993) *Mol. Biol. Cell* **4**, 871–884
- Niessen, C.-M., Hulsman, E. H., Oomen, L. C., Kuikman, I., and Sonnenberg, A. (1997) *J. Cell Sci.* **110**, 1705–1716
- Schaapveld, R. Q., Borradori, L., Geerts, D., van Leusden, M. R., Kuikman, I., Nievers, M. G., Niessen, C. M., Steenbergen, R. D., Snijders, P. J., and Sonnenberg, A. (1998) *J. Cell Biol.* **142**, 271–284
- Dans, M., Gagnoux-Palacios, L., Blaikie, P., Klein, S., Mariotti, A., and Giancotti, F. G. (2001) *J. Biol. Chem.* **276**, 1494–1502
- Marchisio, P. C., Bondanza, S., Cremona, O., Cancedda, R., and De Luca, M. (1991) *J. Cell Biol.* **112**, 761–773
- Niessen, C. M., van der Raaij-Helmer, M. H., Hulsman, E. H., van der Neut, R., Jonkman, M. F., and Sonnenberg, A. (1996) *J. Cell Sci.* **109**, 1695–1706
- Rheinwald, J. G., and Green, H. (1975) *Cell* **6**, 331–344
- Green, H. (1980) *Harvey Lect.*, Series **74**, 101–139
- Pellegrini, G., Golisano, O., Paterna, P., Lambiase, A., Bonini, S., Rama, P., and De Luca, M. (1999) *J. Cell Biol.* **145**, 769–782
- Regnier, M., Schweizer, J., Michel, S., Bailly, C., and Prunieras, M. (1986) *Exp. Cell Res.* **165**, 63–72
- Dellambra, E., Vailly, J., Pellegrini, G., Bondanza, S., Golisano, O., Macchia, C., Zambruno, G., Meneguzzi, G., and De Luca, M. (1998) *Hum. Gene Ther.* **9**, 1359–1370
- Gallio, G. G., O'Connor, N. E., Compton, C. C., Kehinde, O., and Green, H. (1984) *N. Engl. J. Med.* **311**, 448–451
- Pellegrini, G., Traverso, C. E., Franz, A.-T., Zingirian, M., Cancedda, R., and De Luca, M. (1997) *Lancet* **349**, 990–993
- Pellegrini, G., Ranno, R., Stracuzzi, G., Bondanza, S., Guerra, L., Zambruno, G., Micali, G., and De Luca, M. (1999) *Transplantation* **68**, 868–879
- Mathor, M. B., Ferrari, G., Dellambra, E., Cilli, M., Mavilio, F., Cancedda, R., and De Luca, M. (1996) *Proc. Natl. Acad. Sci. U. S. A.* **93**, 10371–10376
- Suzuki, S., and Naitoh, Y. (1990) *EMBO J.* **9**, 757–763
- Miller, D. A., and Rosman, G. J. (1989) *BioTechniques* **7**, 980–988
- Mainiero, F., Murgia, C., Wary, K. K., Curatola, A. M., Pepe, A., Blumemberg, M., Westwick, J. K., Der, C. J., and Giancotti, F. G. (1997) *EMBO J.* **16**, 2365–2375
- Dellambra, E., Golisano, O., Bondanza, S., Siviero, E., Lacal, P., Molinari, M., D'Atri, S., and De Luca, M. (2000) *J. Cell Biol.* **149**, 1117–1129
- Zambruno, G., Marchisio, P.-C., Marconi, A., Vaschieri, C., Melchiori, A., Giannetti, A., and De Luca, M. (1995) *J. Cell Biol.* **129**, 853–865
- Cavani, A., Zambruno, G., Marconi, A., Manca, V., Marchetti, M., and Giannetti, A. (1993) *J. Invest. Dermatol.* **101**, 600–604
- Tidman, M. J., Eady, R. A. (1986) *J. Invest. Dermatol.* **86**, 51–56
- Murgia, C., Blaikie, P., Kim, N., Dans, M., Petrie, H. T., and Giancotti, F. G. (1998) *EMBO J.* **17**, 3940–3951
- Reznicek, G. A., de Pereda, J. M., Reipert, S., and Wiche, G. (1998) *J. Cell Biol.* **141**, 209–225
- Geerts, D., Fontao, L., Nievers, M. G., Schaapveld, R. Q., Purkis, P. E., Wheeler, G. N., Lane, E. B., Leigh, I. M., and Sonnenberg, A. (1999) *J. Cell Biol.* **147**, 417–434
- Hopkinson, S. B., and Jones, J. C. (2000) *Mol. Biol. Cell* **11**, 277–286
- Fuchs, E., and Yang, Y. (1999) *Cell* **98**, 547–550
- Weiss, A., and Littman, D. R. (1994) *Cell* **76**, 263–274